

Supplemental Materials

Molecular Biology of the Cell

O'Neill et al.

Supplemental Information

Contents:

Fig S1: Negative control. mCh-SspB alone does not induce polarity and migration

Fig S2: CXCR4 activation triggers Rac-biosensor translocation in RAW cells

Fig S3: Schematic showing the generation of kymographs

Fig S4: Kymographs showing Cdc42 responses to optical activation of Cdc42 or Rac

Fig S5: Kymographs showing actin responses to optical activation of Cdc42

Fig S6: Kymographs showing Rac1 responses to optical activation of Cdc42 or Rac

Fig S7: Kymographs showing PIP3 responses to optical activation of GPCR, Cdc42, or Rac

Fig S8: Kymographs showing myosinIIA responses to optical activation of Cdc42

Fig S9: Spatiotemporal dynamics of myosinIIA response to Cdc42 activation

Fig S10: Cdc42 activation at the cell front triggers myosinIIB accumulation at the cell rear

Fig S11: MyosinIIA accumulates at the leading edge in a subset of RAW cells

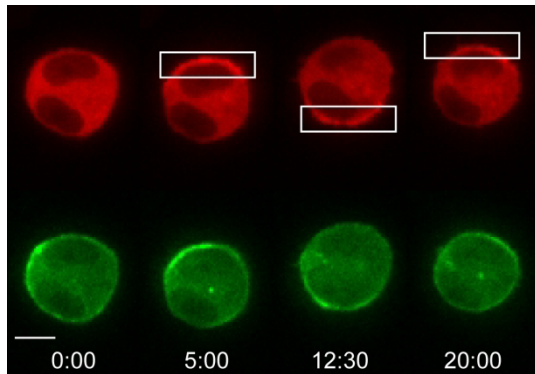


Fig. S1: Negative control. An mCh-SspB construct lacking the Cdc42 GEF domain of ITSN does not generate migratory responses. RAW cell transfected with mCh-SspB, and iLID-CaaX. The SspB construct rapidly translocates to the plasma membrane at the optically activated side of the cell, but unlike ITSN-mCh-SspB it does not generate membrane protrusions or forward migration. Additionally, unlike ITSN-mCh-SspB, optical recruitment to one side of the cell does not generate myosin accumulation at the opposite side. Time is given in min:sec. Scale bar: 10 μ m. Compare to **Fig. 3** and **Fig. 7**.

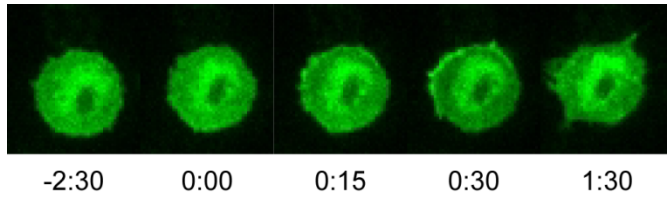


Fig. S2: CXCR4 mediated activation of Rac results in translocation of the Rac biosensor. RAW cell transfected with CXCR4 and the Rac biosensor. CXCR4 was activated with 50 ng/ml SDF-1 α at t=0, resulting in translocation of the Rac biosensor to the plasma membrane.

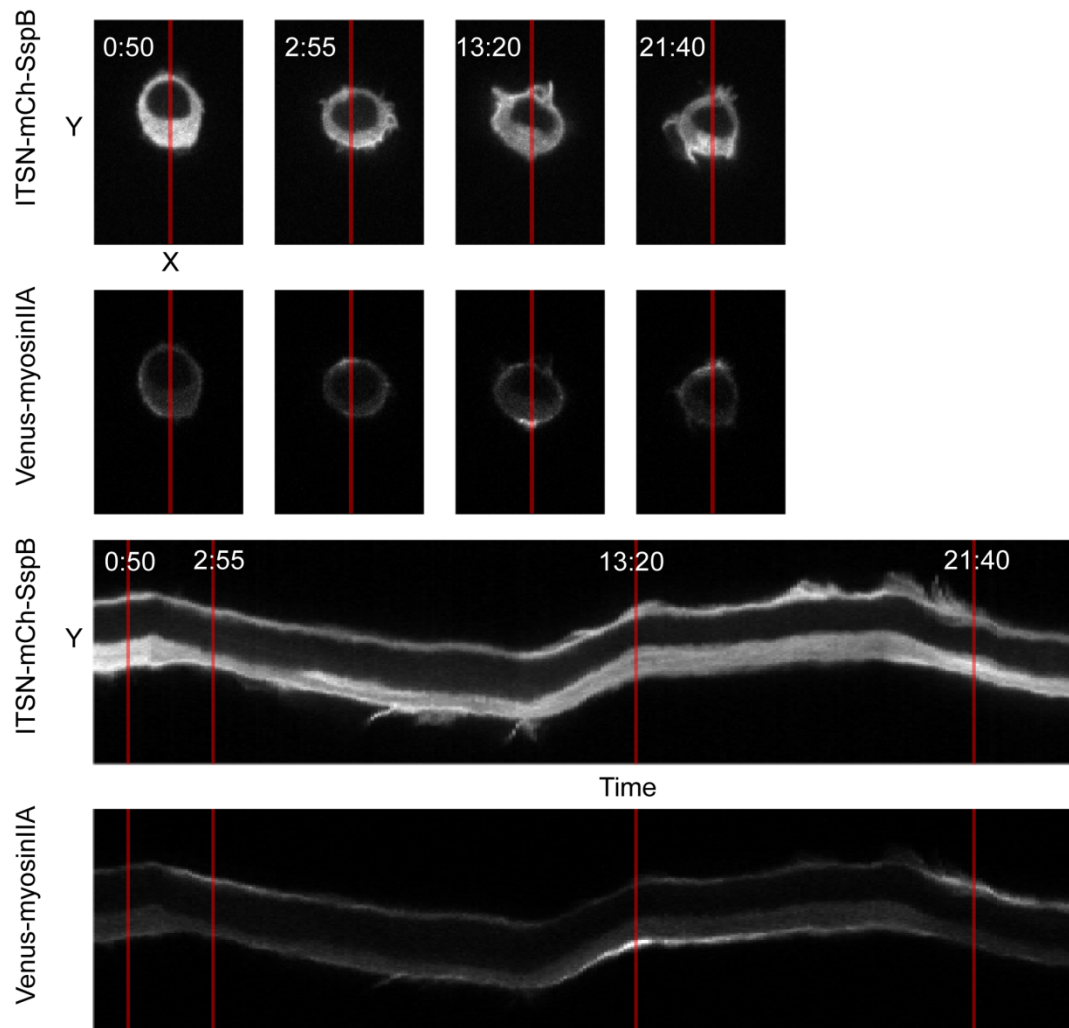
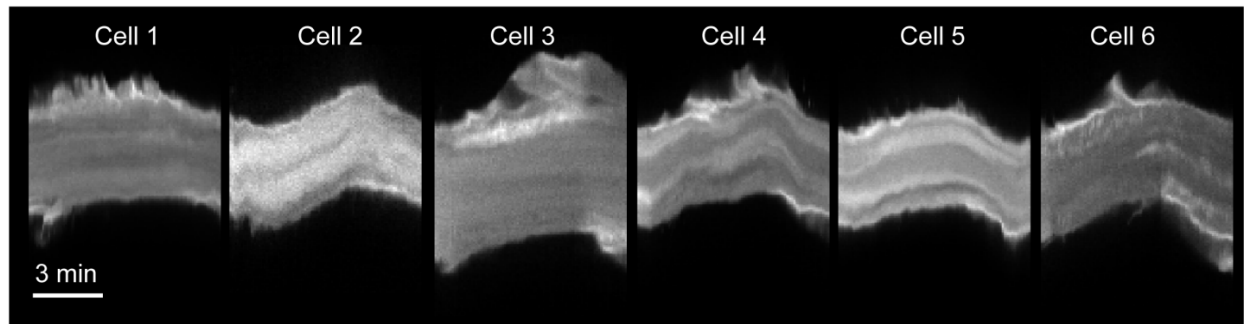


Fig. S3: Kymograph example. Sample data for a single cell demonstrating how kymograph data was generated. A four pixel wide region near the center of the cell was selected (red region), and the intensity was averaged over the width of the region, resulting in a 1D array of intensities for each time point. By showing all of the time point along the horizontal axis, dynamic changes in fluorescent intensity between the front and back of the cell can be quickly identified. The direction of migration can be inferred from the kymograph. In the example shown here, the direction of migration was reversed multiple times by switching the side of optical activation. The kymographs show the cell migrating towards the side with increased ITSN-mCh-SspB, with myosin accumulation at the opposite side.

(A) Cdc42 response to optical activation of Cdc42



(B) Cdc42 response to optical activation of Rac

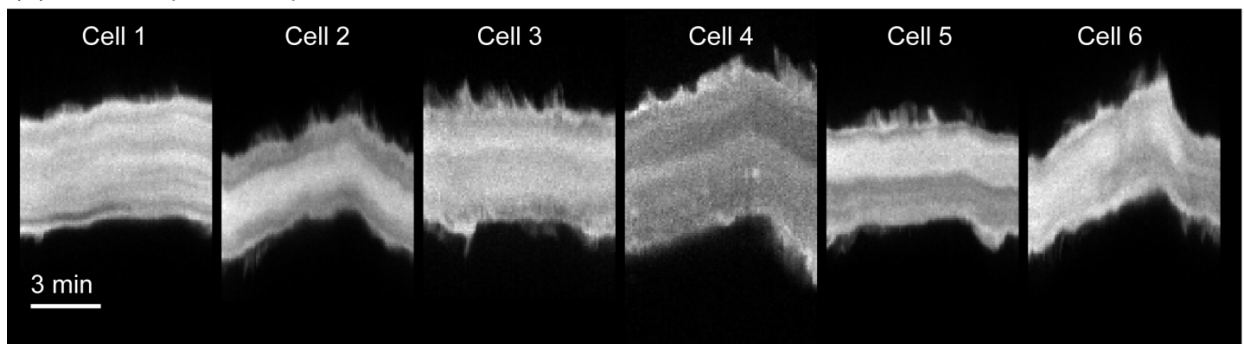


Fig. S4: Kymographs showing the Cdc42 response to optical activation of Cdc42 or Rac. RAW cells were transfected with either (A) ITSN-mCh-SspB or (B) Tiam-mCh-SspB, and iLID-CaaX, Cdc42, and Venus-wGBD (shown).

Actin response to optical activation of Cdc42

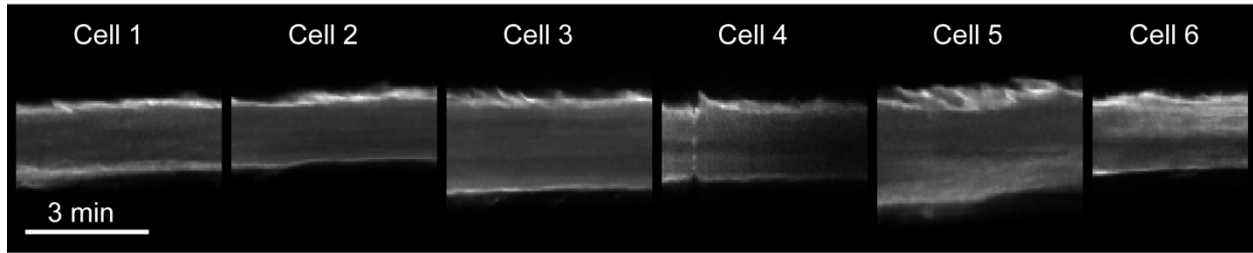
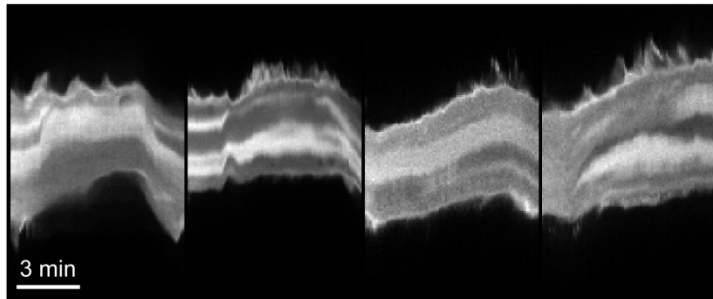


Fig. S5: Kymographs showing the actin response to optical activation of Cdc42. RAW cells were transfected with ITSN-mCh-SspB, iLID-CaaX, and mTopaz-Lifeact (shown).

(A) Rac1 response to optical activation of Cdc42



(B) Rac1 response to optical activation of Rac

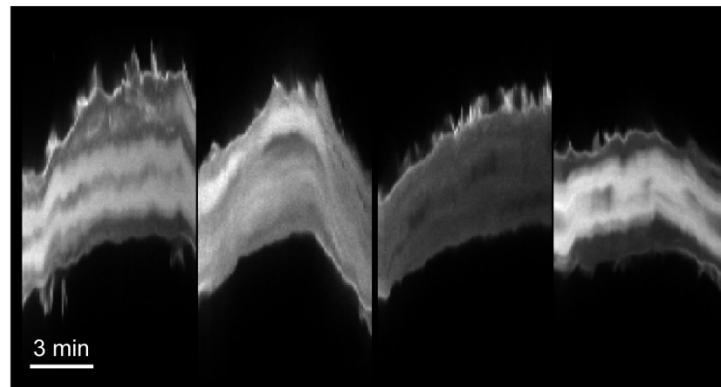
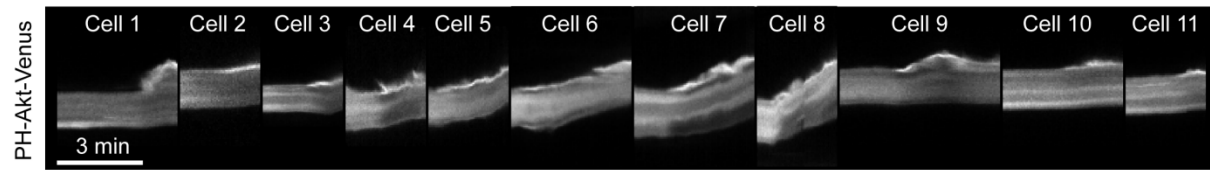
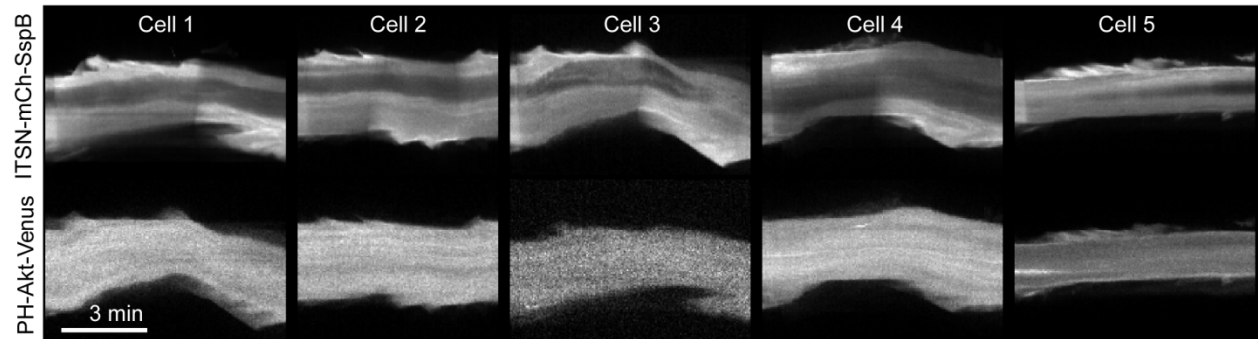


Fig. S6: Kymographs showing the Rac1 response to optical activation of Cdc42 or Rac. RAW cells were transfected with either (A) ITSN-mCh-SspB or (B) Tiam-mCh-SspB, and iLID-CaaX, Cdc42, and Rac1-biosensor (shown).

(A) PIP3 response to optical activation of blue opsin



(B) PIP3 response to optical activation of Cdc42



(C) PIP3 response to optical activation of Rac1

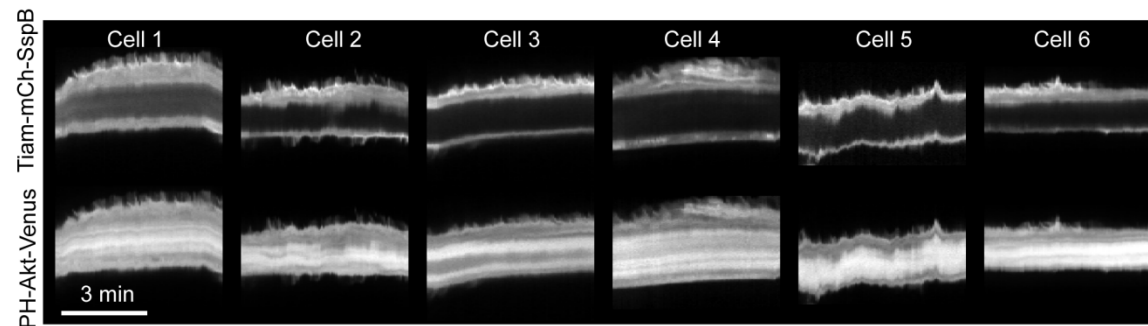


Fig. S7: Kymographs showing the PIP3 response to optical activation of GPCR, Cdc42, or Rac. RAW cells were transfected with PH-Akt-Venus (shown) and the following: (A) blue-opsin-mCherry, (B) ITSN-mCh-SspB + iLID-CaaX, (C) Tiam-mCh-SspB + iLID-CaaX. The kymographs are all oriented such that top corresponds to the initial side of photoactivation. Localized GPCR activation using blue opsin produces steep PIP3 gradients, evident in the PH-Akt-Venus kymographs. In contrast, optically triggered membrane recruitment of ITSN or Tiam does not generate clearly detectable translocation of the PH-Akt domain from the cytosol to the plasma membrane.

MyosinIIA response to optical activation of Cdc42

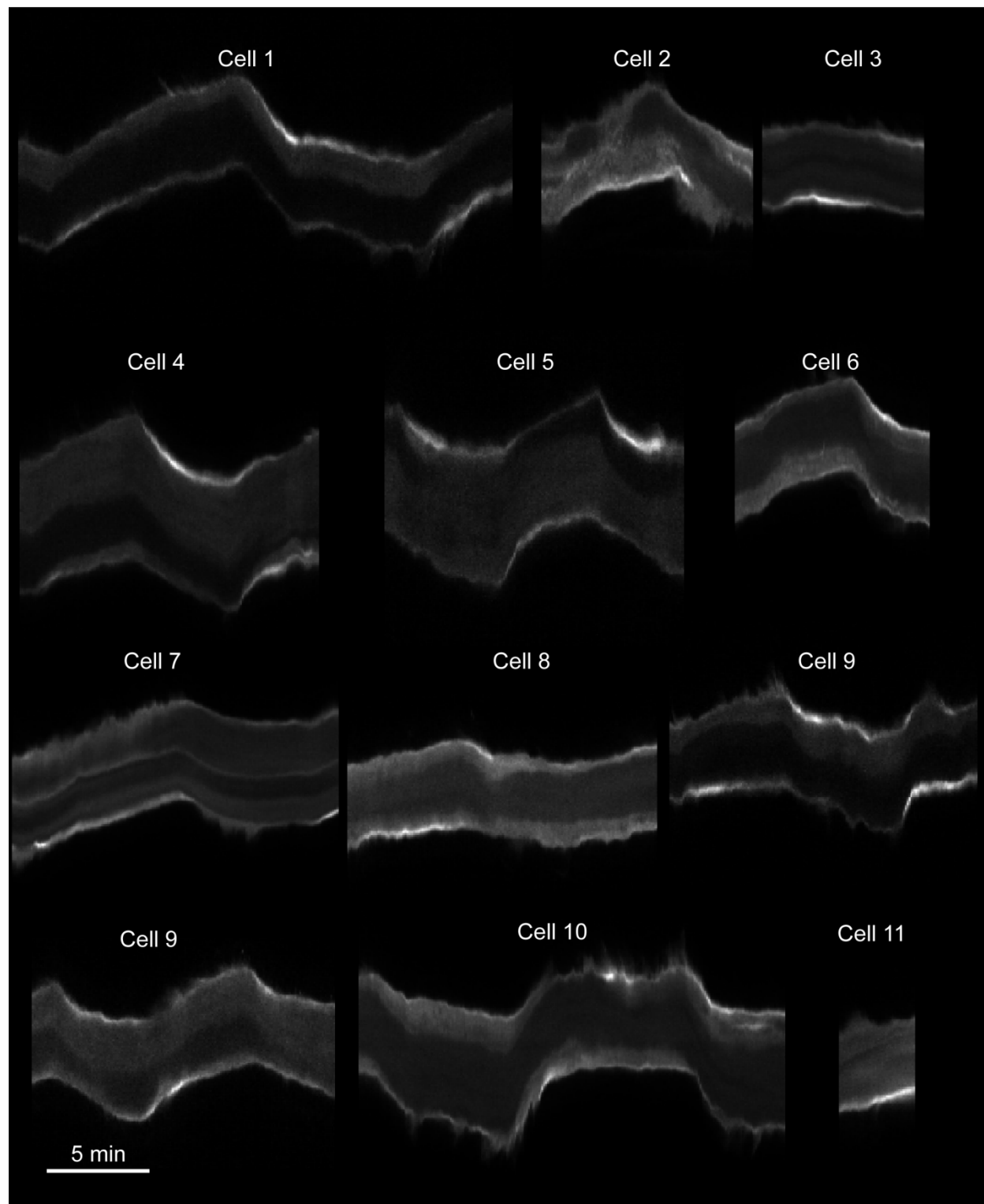


Fig. S8: Kymographs showing the myosinIIA response to optical activation of Cdc42. RAW cells were transfected with either (A) ITSN-mCh-SspB or (B) Tiam-mCh-SspB, and iLID-CaaX, and Venus-myosinIIA (shown).

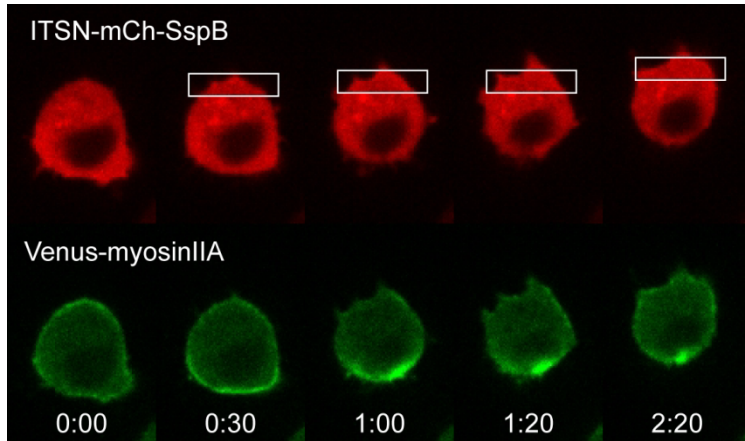


Fig. S9. MyosinIIA dynamics. RAW cell transfected with ITSN-mCh-SspB, iLID-CaaX, and Venus-myosinIIA. Optical activation of Cdc42 at one side of the cell initially generates a crescent of myosinIIA at the opposite side. The crescent then condenses to form a focal spot directly opposite from the side of optical activation.

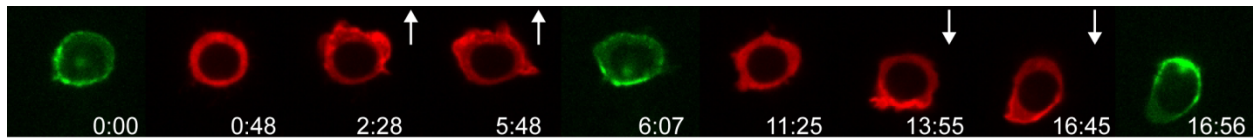


Fig. S10: Cdc42 activity at the cell front triggers myosinIIB accumulation at the rear. RAW cell transfected with ITSN-mCh-SspB, iLID-CaaX, and MHC-IIB-EGFP. Green images show the distribution of myosin IIB. Red images show the distribution of ITSN-mCh-SspB. Myosin IIB localizes to the back of the cell and this reversed upon switching the side of photoactivation. White arrows show the direction of optical activation. Since imaging GFP with 488 nm excitation causes global photoactivation of the entire cell, GFP images were only captured once localized optical activation generated clear directional responses.

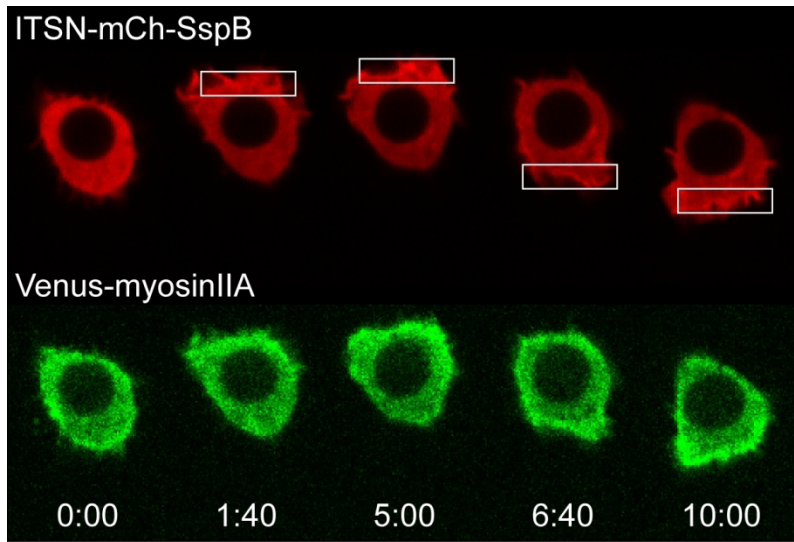


Fig. S11: MyosinIIA accumulates at the leading edge in a subset of RAW cells. RAW cell transfected with ITSN-mCh-SspB, iLID-CaaX, and Venus-myosinIIA. As shown here, optical activation of Cdc42 at one side of the cell resulted in accumulation of myosinIIA at the front of the cell in about 10% of cells (7 of 63 cells). Reversing the side of optical activation resulted in myosinIIA redistribution towards the new leading edge.